Eur. Phys. J. Appl. Phys. (2014) 66: 30101
DOI: 10.1051/epjap/2014140040

THE EUROPEAN PHYSICAL JOURNAL APPLIED PHYSICS

Regular Article

Synthesis and characterization of $Pb(Yb_{1/2}Nb_{1/2})O_3$-based high-Curie temperature piezoelectric ceramics

Jianfeng Zheng[1], Zhihui Chen[1], Bijun Fang[1,a], Jianning Ding[1,2,b], Xiangyong Zhao[3], Haiqing Xu[3], and Haosu Luo[3]

[1] School of Information Science and Engineering, School of Materials Science and Engineering, Changzhou University, Changzhou, Jiangsu 213164, P.R. China
[2] School of Material Science and Engineering, Jiangsu University, Zhenjiang, Jiangsu 212013, P.R. China
[3] Key Laboratory of Inorganic Function Material and Device, Chinese Academy of Sciences, Shanghai 201800, P.R. China

Received: 1 February 2014 / Received in final form: 20 April 2014 / Accepted: 2 May 2014
Published online: 10 June 2014 –

Abstract. xPb$(Yb_{1/2}Nb_{1/2})O_3$-$(1-x)$Pb$(Zr_{0.36}Ti_{0.64})O_3$ (xPYN-$(1-x)$PZT) piezoelectric ceramics were prepared by the conventional ceramic processing via a B-site oxide mixing route. The synthesized xPYN-$(1-x)$PZT ceramics exhibit majority of perovskite structure with slight content of impurity, which exhibit typical tetragonal structure with slight orthorhombic distortion depending on compositions. All the xPYN-$(1-x)$PZT ceramics exhibit high Curie temperature (T_C/T_m), higher than 380 °C, and their dielectric behavior above T_C/T_m can be fitted well by the Curie-Weiss law. The xPYN-$(1-x)$PZT ceramics exhibit large resistivity, and excellent ferroelectric and piezoelectric properties, which provide promising for the high-power and high-temperature piezoelectric applications. However, electric energy density of the xPYN-$(1-x)$PZT ceramics is small due to their nearly rectangular shape of polarization-electric field (P-E) hysteresis loop and early electric displacement saturation, which is not suitable for high energy and power storage applications.

1 Introduction

To meet the requirements of high-power and high-temperature applications, piezoelectric materials with a high ferroelectric phase transition temperature (i.e., the temperature of dielectric constant maximum, T_C/T_m) and a high vibration velocity have attracted great research attention [1–3]. Relaxor-based ferroelectric solid solutions provide advantage research hotspot due to their versatile composition selection, in which $(1-x)PbZrO_3$-$xPbTiO_3$ (PZT)-based compositions are well-known piezoelectric materials for such applications, whereas T_C/T_m and piezoelectric property need further improving [4].

The discovery of novel materials with innovative properties always promotes a technological breakthrough. $Pb(Yb_{1/2}Nb_{1/2})O_3$ (PYN) is a compositionally ordered antiferroelectric, which exhibits a monoclinic perovskite structure with T_C around 300 °C [5,6]. A morphotropic phase boundary (MPB) forms in the PZT system, where two similar ferroelectric phases with equivalent energy state coexist, leading to enhanced crystal structure and improved electrical properties [7,8]. Therefore, forming solid solutions with perovskite structure provide opportunities to tailor electrical properties [9,10] since the arrangement of heterovalent cations and their electrostatic interactions on the B-site of the perovskite structure change greatly, which influence dielectric behavior and electromechanical response and provide promising research directions [11,12].

In this work, the pseudo-ternary $Pb(Yb_{1/2}Nb_{1/2})O_3$-$PbZrO_3$-$PbTiO_3$ (PYN-PZ-PT) system was studied, which was expected to exhibit high T_C/T_m and piezoelectricity since T_C of PYN (300 °C) is higher than that of $PbZrO_3$ (230 °C) and the end components exhibit similar perovskite structure [13]. To increase T_C/T_m further, the composition of PZT was chosen slight far from the MPB composition, being $Pb(Zr_{0.36}Ti_{0.64})O_3$, which would sacrifice piezoelectric property slightly [8]. Therefore, the influences of sintering conditions and composition on crystal structure and electrical properties of the xPb$(Yb_{1/2}Nb_{1/2})O_3$-(1-x)Pb$(Zr_{0.36}Ti_{0.64})O_3$ (xPYN-$(1-x)$PZT) piezoelectric ceramics were studied systematically. The high content of $PbTiO_3$ was an important factor to obtain high T_C/T_m temperature. The B-site oxide mixing route [14,15] and raw-oxides-mixing-powder burying were used to minimize the evaporation of PbO during sintering, which produces A-site vacancies and deteriorates electrical properties of the synthesized piezoelectric ceramics.

[a] e-mail: fangbj@sohu.com
[b] e-mail: dingjn@cczu.edu.cn

2 Experimental procedure

The xPYN-$(1-x)$PZT piezoelectric ceramics were prepared by the conventional ceramic processing via the B-site oxide mixing route [14,15], in which stoichiometrically mixed B-site oxides, Yb_2O_3, Nb_2O_5, ZrO_2 and TiO_2 were pre-calcined at 1050 °C for 4 h, without the synthesis of the wolframite precursor $YbNbO_4$. The weight of the synthesized B-site precursors was introduced into batch calculation. Stoichiometric PbO was added into the synthesized B-site precursors after careful grinding, and the well mixed powders were calcined at 850 °C for 2 h. The calcined powders were then cold dry-pressed into pellets with the addition of 1.5 wt.% polyvinyl alcohol (PVA) binder and sintered at 1200–1250 °C for 2 h. The green pellets were buried under an equiweight mixture of raw oxides with the same composition in a covered crucible to minimize the evaporation of lead during sintering. No additional PbO was added for the preparation of the xPYN-$(1-x)$PZT ceramics.

The sintered xPYN-$(1-x)$PZT ceramics were ground and polished to obtain flat and parallel surfaces. Crystal structure of the sintered xPYN-$(1-x)$PZT ceramics was measured by a Rigaku D/max-2500/PC X-ray diffractionmeter (XRD, Rigaku Corporation, Japan) using Cu Kα radiation. For electrical properties measurements, silver paste was coated on both surfaces of the well-polished ceramics and fired at 600 °C for 20 min to provide robust electrodes. Dielectric property was measured by a computer-controlled TH2818 Automatic Component Analyzer under a weak oscillation level of 1 V_{rms} (Changzhou Tonghui Electronic Co. Ltd., China) combining with a programmable furnace. Polarization-electric field (*P-E*) hysteresis loop was characterized by a Radiant Precision Premier LC ferroelectric material test system (Radiant Technologies Inc., USA). For piezoelectric property measurement, the ceramics were poled under an electric field of 6 kV/mm at 100 °C for 15 min in silicon oil. Piezoelectric property was measured by a ZJ-6A Berlincourt-type quasi-static d_{33}/d_{31} meter (Institute of Acoustics, Chinese Academy of Sciences, China). Detailed electrical properties measurement procedures were described elsewhere [11].

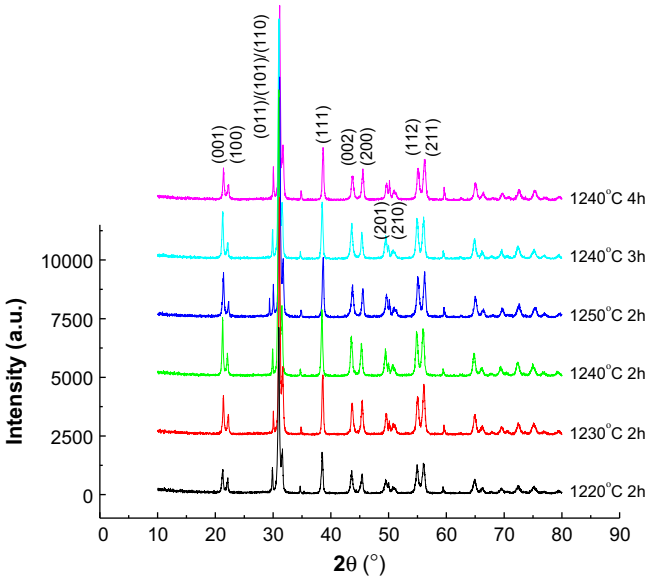

Fig. 1. XRD patterns of the 0.075PYN-0.925PZT ceramics sintered at different temperatures for different times.

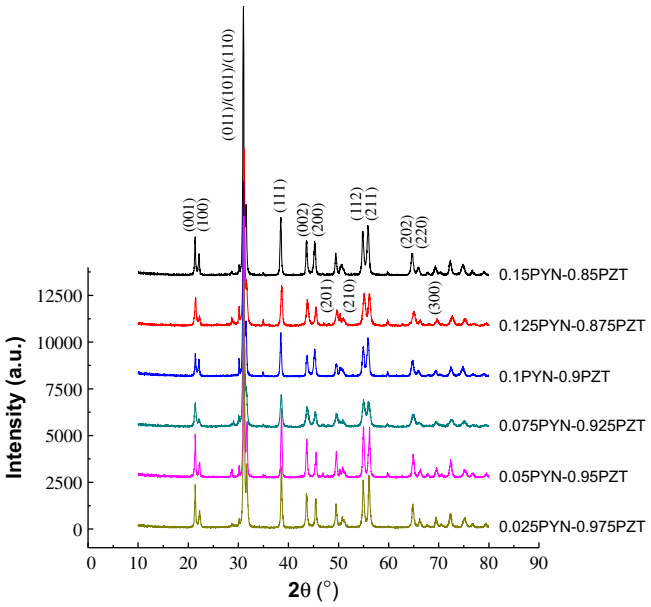

Fig. 2. XRD patterns of the xPYN-$(1-x)$PZT ceramics sintered at 1240 °C for 2 h.

3 Results and discussion

Figure 1 shows XRD patterns of the 0.075PYN-0.925PZT ceramics sintered at different temperatures. For different sintering temperatures and times, the sintered 0.075PYN-0.925PZT ceramics exhibit majority of perovskite structure with slight content of undetermined impurity around 2θ of 35° and 60°. The amount of impurity tends to increase slightly with the increase of sintering temperature and time. It can be seen from these XRD patterns, {1 0 0}, {2 0 0}, {2 1 0}, etc. crystal faces exhibit typically tetragonal doubly splitting, and {3 0 0}, {3 1 0}, {3 1 1} diffraction reflections broaden apparently, whereas {1 1 0} crystal face exhibits orthorhombic triple splitting. Such phenomena indicate that the sintered 0.075PYN-0.925PZT ceramics exhibit tetragonal perovskite structure but with slight orthorhombic crystal distortion.

Figure 2 shows XRD patterns of the xPYN-$(1-x)$PZT ceramics sintered at relatively appropriate sintering conditions. To determine the phase formation clearly, the XRD patterns around the {2 0 0} diffraction reflection with 2θ = 43–46° is shown in Figure 3. All these compositions exhibit rather typical tetragonal perovskite structure, in which slight content of pyrochlore phase and undetermined impurity forms, and crystal distortion appears. With the increase of the PYN content, the characteristics of tetragonal splitting, diffraction peaks'

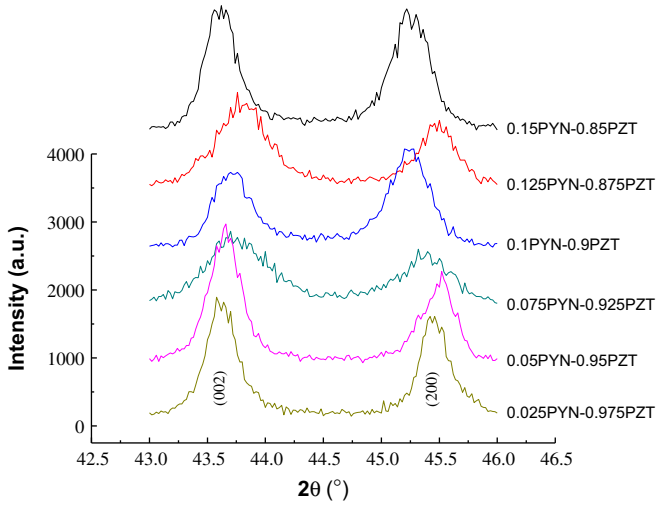

Fig. 3. XRD patterns around the {2 0 0} diffraction reflection of the xPYN-$(1-x)$PZT ceramics.

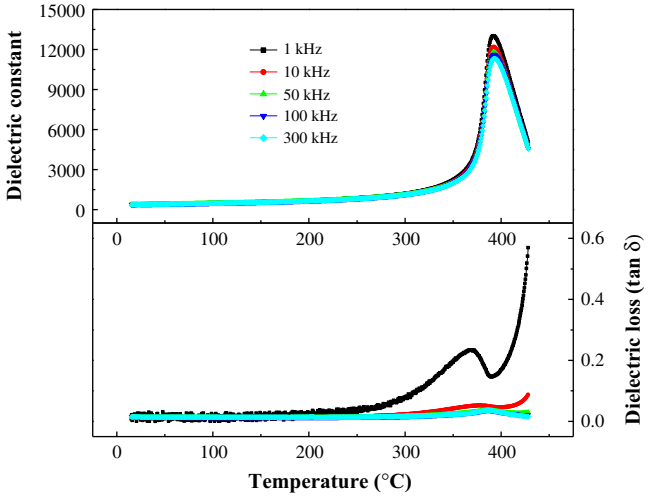

Fig. 4. Temperature dependence of dielectric constant and loss tangent of the 0.075PYN-0.925PZT ceramics sintered at 1240 °C for 2 h measured at several frequencies.

symmetry, relative intensity and width, and the calculated tetragonality (defined as the ratio of cell parameter c/a) change accompanied by the displacement of diffraction peaks, but do not exhibit apparent regularity. Based on the XRD results and bulk density measurement, the optimized sintering conditions can be determined primarily although sintering conditions should be tailored further for each compositions. The 0.075PYN-0.925PZT ceramics sintered at 1240 °C for 2 h exhibit the largest relative density, being 96.7%, in which the bulk density is 7.638 g/cm^3, and the cell parameters are $a = b = 4.0386(481)$ Å, $c = 4.1669(653)$ Å, and $V_{\text{cell}} = 67.964$ Å^3 calculated by the Wincell version 1.1 software (written by Fazil A. Rajaballee) using $2\theta =$ 10–80° X-ray diffraction peaks.

Figure 4 shows temperature dependence of dielectric property of the 0.075PYN-0.925PZT ceramics sintered at

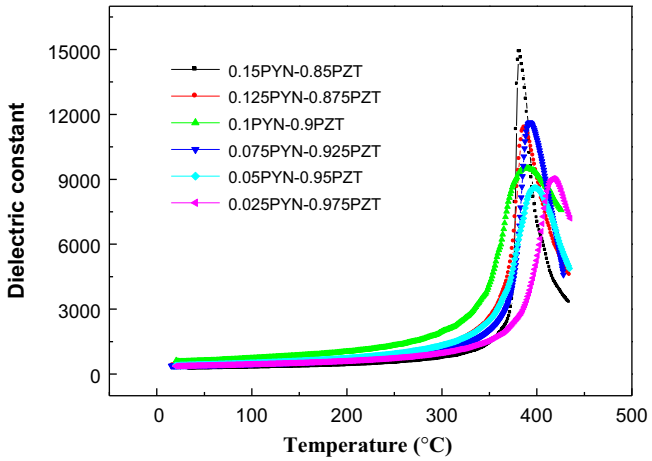

Fig. 5. Temperature dependence of dielectric constant of the xPYN-$(1-x)$PZT ceramics sintered at 1240 °C for 2 h measured at 100 kHz.

relatively optimized conditions. Due to the large content of $PbTiO_3$ in the solid solution, the 0.075PYN-0.925PZT ceramics exhibit large T_C/T_m temperature, being 392.2 °C, which corresponds well to that determined by the linear combination rule using the T_C/T_m temperatures of the three end components. Its room-temperature dielectric loss is small, which increases greatly around the temperatures of T_C/T_m. Therefore, further improvements, such as composition adjustment, doping and tailoring sintering conditions, are needed to meet the requirements of the high-power and high-temperature piezoelectric applications. The dielectric-response peaks are sharp and narrow, and the dielectric behavior above the T_C/T_m temperature can be fitted well by the Curie-Weiss law $\varepsilon = C/T - T_0$ in the temperature range measured, indicating that the ferroelectric phase transition (FPT) from tetragonal ferroelectric phase to cubic paraelectric phase is a first-order FPT similar to that of the normal ferroelectrics [16]. Since the 0.075PYN-0.925PZT ceramics is a solid solution, slight dielectric frequency dispersion appears around the T_C/T_m temperature and less than 1 °C ΔT_m occurs between 1 and 300 kHz. Therefore, the 0.075PYN-0.925PZT ceramics cannot be a typical normal ferroelectric. The abnormal increase of dielectric loss above T_C/T_m at low frequency 1 kHz, similar to that of the Fe-containing lossy ferroelectrics [17], cannot be interpreted now.

Figure 5 shows temperature dependence of dielectric constant of the xPYN-$(1-x)$PZT ceramics measured at 100 kHz. In order to obtain piezoelectric materials for high-temperature applications, all these compositions possess tetragonal perovskite structure, therefore, their dielectric behavior exhibits characteristic similar to that of the normal ferroelectrics on the whole. At room-temperature, their relative dielectric constant is around 230–630 and exhibits increase tendency with the increase of the PZT content. All the synthesized xPYN-$(1-x)$PZT ceramics exhibit narrow and sharp dielectric-response peaks, and their dielectric behavior above the T_C/T_m temperatures can be fitted well by the Curie-Weiss law

$\varepsilon = C/T - T_0$ with different values of Curie-Weiss constant C and Curie-Weiss temperature T_0 except the 0.1PYN-0.9PZT ceramics whose dielectric-response peaks are slightly broad. With the increase of the PZT content, the T_C/T_m temperature increases almost linearly and all higher than 380 °C, which provides possibility for the applications of high-temperature transducers and capacitors. The xPYN-$(1-x)$PZT ceramics also exhibit peak maximum value of dielectric loss at temperatures lower than their T_C/T_m temperatures. However, the shape and width of the dielectric-response peaks, and the values of dielectric constant maximum (ε_m) exhibit no apparent regularity.

Figure 6 shows *P-E* hysteresis loop of the 0.075PYN-0.925PZT ceramics measured at room temperature. At 1 Hz and 55 kV/cm, the sintered 0.075PYN-0.925PZT ceramics exhibit fully developed, saturated and symmetric hysteresis loop. The hysteresis loop is broad and exhibits nearly rectangular shape accompanied by large value of coercive field E_c, which can be attributed to its crystal structure nature, i.e., tetragonal perovskite structure. The closed and saturated hysteresis loop seems to be intrinsic and relates to its low dielectric loss. No apparent pinning-down effect appears, indicating that crystal defects are small in the synthesized ceramics [18]. Based on the fully saturated *P-E* hysteresis loop, ferroelectric properties of remnant polarization P_r and E_c can be determined, being 16.81 μC/cm^2 and 39.14 kV/cm, respectively. The ceramics also exhibit large resistivity, being 1.019×10^{10} Ω cm, which can be applied large direct electric field for polarization to induce excellent piezoelectric properties. Mean value of piezoelectric constant d_{33} is 268 pC/N. The ceramics exhibit perfect resonance response peaks in the radial-extension-vibration-mode, where the calculated electromechanical coupling factors $K_p \approx \sqrt{\frac{f_p - f_s}{f_s}} \times 2.51$ and mechanical equality factor $Q_m = \frac{f_p^2}{2\pi \times f_s \times C^T \times R(f_p^2 - f_s^2)}$ are 0.442 and 175, respectively. However, for high-power piezoelectric applications, the value of Q_m need increase further.

For high energy and power storage applications, a high electric breakdown field E_b, a high electric displacement or charge density D and a proper dielectric constant ε are key factors to achieve high energy density [19]. Electric energy density of the 0.075PYN-0.925PZT ceramics can be calculated by integrating the colored area of the *P-E* loop (Fig. 6), being 0.26 J/cm^3 under 55 kV/cm, which is rather small as compared with biaxially oriented polypropylene whose energy density is ~4 J/cm^3 under 6000 kV/cm [19]. Such phenomenon can be attributed to the effect of the early electric displacement D-saturation, in which external applied electric field just induces small change in D between P_r and saturation polarization P_s, then leading to low energy density [20]. The discharged energy density varies with the electric field E as shown in Figure 7 since E influences ferroelectric property greatly. The discharged energy density of the 0.075PYN-0.925PZT ceramics increases in an exponential fashion with E, which is different from that of the dielectric polymer whose energy density increases linearly with E or proportional to the square of E [19]. However, due to the saturation characteristic of the *P-E* loop and not large value of E_b, the 0.075PYN-0.925PZT ceramics cannot achieve higher energy density by just raising electric field. Therefore, increasing D via tailoring composition or doping to obtain slim shape *P-E* loop without early D-saturation and raising E_b by improving ceramic quality with proper dielectric constant may be effective approaches to achieve high energy density ferroelectric ceramics for modern electronic and electric power systems.

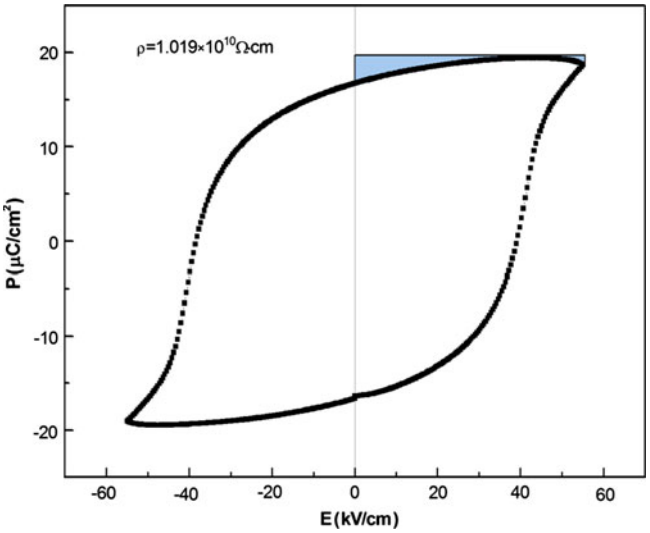

Fig. 6. Room-temperature *P-E* ferroelectric hysteresis loop of the 0.075PYN-0.925PZT ceramics sintered at 1240 °C for 2 h measured at 1 Hz.

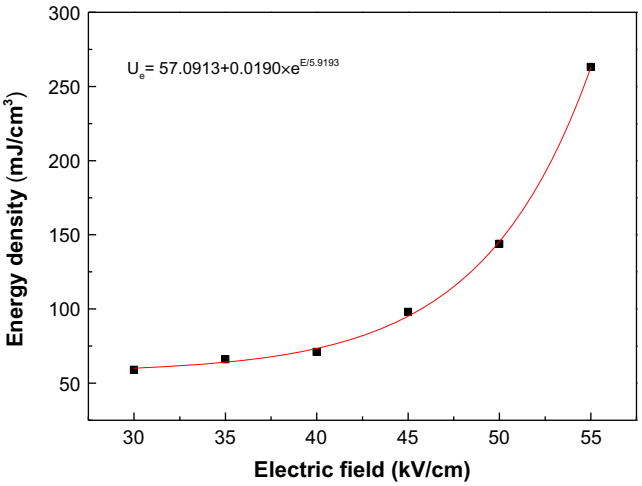

Fig. 7. The discharged energy density as a function of the electric field amplitude of the 0.075PYN-0.925PZT ceramics measured from the *P-E* loops. The solid curve is exponential fitting of the data. The fitting equation is shown in the plot.

4 Conclusions

The xPYN-$(1-x)$PZT piezoelectric ceramics were prepared by the solid-state reaction method via the B-site

oxide mixing route. The synthesized xPYN-$(1-x)$PZT ceramics exhibit tetragonal perovskite structure with slight orthorhombic distortion, in which impurity content, tetragonality and crystal distortion change with composition. All the xPYN-$(1-x)$PZT ceramics exhibit nearly normal ferroelectric phase transition, in which the dielectric-response peaks are narrow, sharp and almost frequency independent, and their dielectric behavior above T_C/T_m can be fitted well by the Curie-Weiss law. The xPYN-$(1-x)$PZT ceramics exhibit high Curie temperature, all higher than 380 °C, and increase almost linearly with the increase of the PZT content. The xPYN-$(1-x)$PZT ceramics exhibit high density, large resistivity and excellent electrical properties, in which the 0.075PYN-0.925PZT ceramics sintered at 1240 °C for 2 h show relative density 96.7%, resistivity 1.019×10^{10} Ω cm, T_C 392.2 °C, P_r 16.81 $\mu C/cm^2$, d_{33} 268 pC/N, K_p 0.442 and electric energy density 0.26 J/cm^3. Such excellent ferroelectric and piezoelectric properties make the xPYN-$(1-x)$PZT ceramics promising for the high-power and high-temperature piezoelectric applications.

The authors thank the National Natural Science Foundation of China (Grant Nos. 51242006, 51342002), the Key Laboratory of Inorganic Function Material and Device, Chinese Academy of Sciences (Grant No. KLIFMD-2011-02) and the Priority Academic Program Development of Jiangsu Higher Education Institutions for financial support.

References

1. J. Ryu, S. Priya, K. Uchino, Appl. Phys. Lett. **82**, 251 (2003)
2. R.E. Eitel, C.A. Randall, T.R. Shrout, P.W. Rehrig, W. Hackenberger, S.-E. Park, Jpn J. Appl. Phys. **40**, 5999 (2001)
3. D.-Y. Jeong, J. Ryu, D.-S. Park, Mater. Sci. Eng. B **163**, 88 (2009)
4. B. Jaffe, R.S. Roth, S. Marzullo, J. Appl. Phys. **25**, 809 (1954)
5. J.R. Kwon, W.K. Choo, J. Phys.: Condens. Matter **3**, 2147 (1991)
6. S.J. Zhang, L. Laurent, S. Rhee, C.A. Randall, T.R. Shrout, Appl. Phys. Lett. **81**, 892 (2002)
7. B. Jaffe, W.R. Cook, H. Jaffe, *Piezoelectric Ceramics* (Academic Press, London, 1971)
8. B. Noheda, J.A. Gonzalo, L.E. Cross, R. Guo, S.-E. Park, D.E. Cox, G. Shirane, Phys. Rev. B **61**, 8687 (2000)
9. L. Ai, X. Li, Z. Wang, Y. Liu, C. He, T. Li, T. Chu, D. Pang, H. Tailor, X. Long, J. Eur. Ceram. Soc. **33**, 2155 (2013)
10. H. Chen, C. Fan, Mater. Lett. **64**, 654 (2010)
11. B. Fang, M. Wang, N. Yuan, J. Ding, X. Zhao, H. Xu, H. Luo, Chin. Sci. Bull. **58**, 4064 (2013)
12. T.R. Shrout, S.L. Swartz, M.J. Haun, Am. Ceram. Soc. Bull. **63**, 808 (1984)
13. W.M. Zhu, Z.-G. Ye, Ceram. Int. **30**, 1443 (2004)
14. S.L. Swartz, T.R. Shrout, Mater. Res. Bull. **17**, 1245 (1982)
15. B. Fang, R. Sun, Y. Shan, K. Tezuka, H. Imoto, J. Mater. Sci. **42**, 9227 (2007)
16. K. Uchino, S. Nomura, Ferroelectr. Lett. **44**, 55 (1982)
17. K.B. Park, K.H. Yoon, Ferroelectrics **145**, 195 (1993)
18. Z.-G. Ye, Curr. Opin. Solid State Mater. Sci. **6**, 35 (2002)
19. B. Chu, X. Zhou, K. Ren, B. Neese, M. Lin, Q. Wang, F. Bauer, Q.M. Zhang, Science **313**, 334 (2006)
20. Q.M. Zhang, V. Bharti, G. Kavarnos, in *The Encyclopedia of Smart Materials*, vol. 2, edited by M. Schwartz (Wiley, New York, 2002)